



Citation: G. Inesi (2019) Similarities and contrasts in the structure and function of the calcium transporter ATP2A1 and the copper transporter ATP7B. *Substantia* 3(1): 9-17. doi: 10.13128/Substantia-68

Copyright: © 2019 G. Inesi. This is an open access, peer-reviewed article published by Firenze University Press (<http://www.fupress.com/substantia>) and distributed under the terms of the Creative Commons Attribution License, which permits unrestricted use, distribution, and reproduction in any medium, provided the original author and source are credited.

Data Availability Statement: All relevant data are within the paper and its Supporting Information files.

Competing Interests: The Author(s) declare(s) no conflict of interest.

Research Article

Similarities and contrasts in the structure and function of the calcium transporter ATP2A1 and the copper transporter ATP7B

GIUSEPPE INESI

California Pacific Medical Center Research Institute, 32 Southridge Rd West, Tiburon CA 94920, USA

E-mail: giuseppeinesi@gmail.com

Abstract. Ca^{2+} and Cu^{2+} ATPases are enzyme proteins that utilize ATP for active transport of Ca^{2+} or Cu^{2+} across intracellular or cellular membranes.¹⁻⁴ These enzymes are referred to as P-type ATPases since they utilize ATP through formation of a phosphorylated intermediate (E-P) whose phosphorylation potential affects orientation and affinity of bound cations by means of extended conformational changes. Thereby specific cations are transported across membranes, forming transmembrane gradients in the case of Ca^{2+} , or accepting Cu^{2+} from delivering proteins on one side of the membrane and releasing it to carrier proteins on the other side. Binding of Ca^{2+} or Cu^{2+} is required for enzyme activation and utilization of ATP by transfer of ATP terminal phosphate to a conserved aspartate residue. The ATPase protein is composed of a transmembrane region composed of helical segments and including the cation binding site (TMBS), and a cytosolic headpiece with three domains (A, N and P) containing the catalytic and phosphorylation site. The number of helical segments and the cytosolic headpieces present significant differences in the two enzymes. In addition, details of transmembrane cation extrusion are different. The Ca^{2+} and Cu^{2+} ATPase sustain vital physiological functions, such as muscle contraction and relaxation, activation of several cellular enzymes, and elimination of excess cation concentrations. A historic review of studies on chemical and physiological mechanisms of the Ca^{2+} and Cu^{2+} ATPase is presented.

Keywords. Calcium ATPase, Copper ATPase, Cation Active Transport.

THE CALCIUM TRANSPORT ATPASE

The Ca^{2+} ATPase (SERCA) is a mammalian membrane bound protein sustaining Ca^{2+} transport and involved in cell Ca^{2+} signaling and homeostasis. It is made of a single polypeptide chain of 994 amino acid residues distributed in ten trans-membrane segments (M1 – M10) and a cytosolic headpiece including three distinct domains (A, N and P) that are directly involved in catalytic activity (Fig 1).⁵

The N domain contains residues such (Phe-487) interacting with the adenosine moiety of ATP whereby the ATP substrate is cross-linked to the P domain.

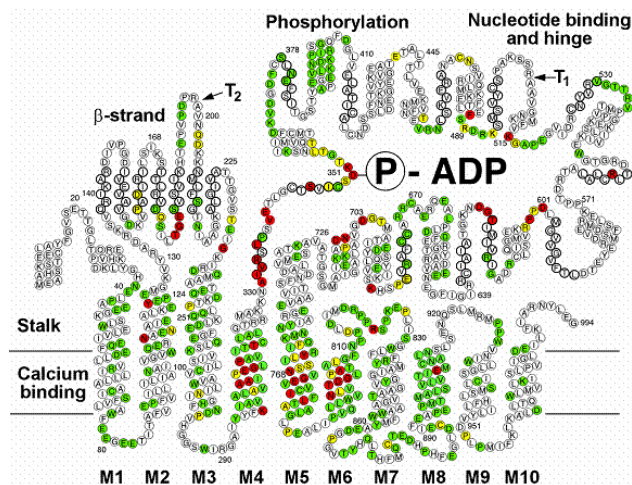


Figure 1. Amino acid sequence and two dimensional folding model of the SERCA1 Ca^{2+} ATPase.⁵ See text for explanations.

The P domain contains a residues (Asp-351) undergoing phosphorylation to yield a phosphorylated intermediate (E-P), a residue (Asp-703) coordinating Mg^{2+} , and other features characteristic of P-type ATPases. The A domain contains the signature sequence ^{181}TGE that provides catalytic assistance for final hydrolytic cleavage of (E-P). Cooperative and sequential binding of Ca^{2+} involved in catalytic activation and transport (Figs. 1 and 3) occurs on sites I and II located within the trans-membrane region.^{6,7}

Ca^{2+} ATPases (SERCA1 and SERCA2) are associated with intracellular membranes of skeletal and cardiac muscle (sarcoplasmic reticulum: SR), and especially high concentrations with the skeletal muscle SR. Therefore, isolation of vesicular fragments of skeletal SR yields concentrated and fairly pure protein, shown by very frequent particles corresponding to ATPase protein visualized by electron microscopy (Fig 2 left panel), and prominent ATPase component visualized by electrophoresis (Fig 2, right panel).

This preparation is very convenient for functional and structural characterization of the ATPase.⁸ In fact, it was demonstrated (8) with this preparation that, at equilibrium and in the absence of ATP, SERCA binds two Ca^{2+} per mole, with high cooperativity and high affinity ($2.3 \times 10^6 \text{ M}^{-1}$) (Fig. 3a) at neutral pH, although the affinity is lower at low pH and higher at higher pH.⁹ When ATP is added to SR vesicles pre-incubated with Ca^{2+} in rapid kinetic experiments (Fig 3b), the bound Ca^{2+} facing the outer medium disappears soon (becomes non available to isotopic exchange, i.e., occluded), indicating that the outer opening of the binding cavity closes to the outside medium as soon as a first reaction product with ATP is formed.

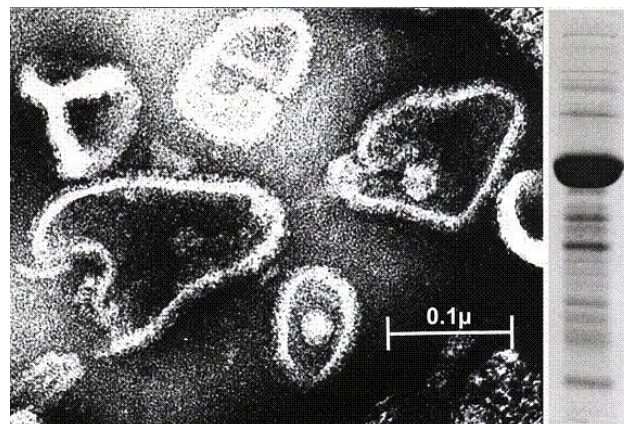


Figure 2. Purified vesicular fragments of sarcoplasmic reticulum membrane shown by negative staining on electron microscopy. On the right side, electrophoretic analysis demonstrates that the protein composition consists almost entirely of Ca^{2+} ATPase.⁸

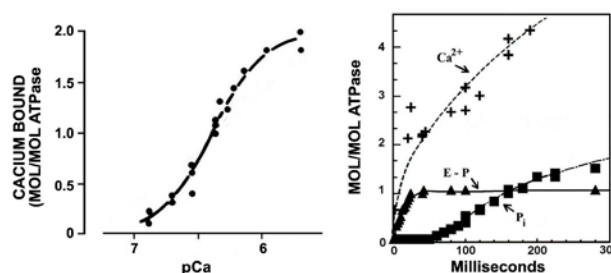


Figure 3a. Ca^{2+} binding to SR ATPase under equilibrium conditions, in the absence of ATP. The stoichiometry of binding is 2 Ca^{2+} per ATPase, with a binding constant of $2.3 \times 10^6 \text{ M}^{-1}$, and high cooperativity.⁹ Figure 3b. Pre-steady state activity of SR vesicles started by addition of ATP in the presence of Ca^{2+} . Note that upon addition of ATP a rapid burst of EP formation occurs and, at the same time, 2 Ca^{2+} per ATPase become occluded. Steady state P_i production and further Ca^{2+} uptake then follow, with a ratio of 2 Ca^{2+} per P_i produced.¹⁰

P_i release and further Ca^{2+} uptake then occur following a delay, indicating that trans-membrane Ca^{2+} release and hydrolytic cleavage of EP occur after a slow step and, soon after that, further cycles contribute to steady state activity.¹⁰

Based on these kinetic observations, a diagram is shown in Fig. 4, where the basal enzyme is indicated as $2\text{H}^+ \cdot \text{E}_2$. Following 2Ca^{2+} binding in exchange for 2H^+ , the active enzyme is referred to as $\text{E}_1 \cdot 2\text{Ca}^+$. Following the binding and utilization of ATP, the resulting phosphoenzyme is indicated as $\text{ADPE}_1 \cdot \text{P}_2 \cdot \text{Ca}^{2+}$. Upon release of ADP, the free energy associated with this intermediate is utilized for a slow conformational change yielding trans-membrane release of bound Ca^{2+} in exchange for 2H^+ ,

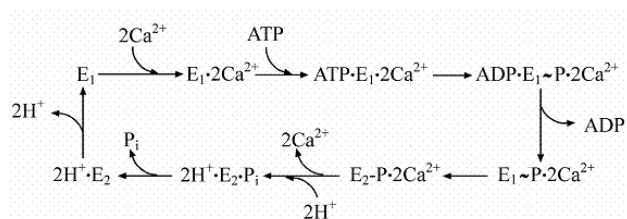


Figure 4. Diagram outlining the sequential reactions of a Ca^{2+} ATPase cycle at neutral pH. The cycle starts with the enzyme in basal conformation, with H^+ bound at the specific Ca^{2+} exchange site ($2\text{H}^+\cdot\text{E}_2$). Upon H^+ dissociation, 2Ca^{2+} bind and the enzyme is activated ($\text{E}_1\cdot 2\text{Ca}^{2+}$). ATP then leads to formation of the high potential phosphorylated intermediate ($\text{ADP}\cdot\text{E}_1\sim\text{P}\cdot 2\text{Ca}^{2+}$). Following dissociation of ADP, the phosphorylated intermediate uses its potential for a conformational change reducing affinity and orientation of bound calcium. 2Ca^{2+} are then dissociated in exchange for 2H^+ . The residual phosphoenzyme then undergoes hydrolytic cleavage with release of P_i , and returns to the basal conformation with H^+ bound ($2\text{H}^+\cdot\text{E}_2$). The stoichiometry of H^+ binding is 2 per E at neutral pH. At high pH, less or no H^+ exchanges for Ca^{2+} . Thereby Ca^{2+} is not released before P_i cleavage, and the enzyme undergoes an uncoupled cycle.

followed by hydrolytic cleavage of P_i and return to the basic $2\text{H}^+\cdot\text{E}_2$ state.

The reaction scheme in Fig. 4 outlines a specific exchange of 2Ca^{2+} for 2H^+ in the $2\text{H}^+\cdot\text{E}_2$ state and 2H^+ for 2Ca^{2+} in the $\text{E}_2\sim\text{P}\cdot 2\text{Ca}^{2+}$ state.

Clear evidence for this exchange was obtained with SERCA reconstituted in phospholipids vesicles that do not allow trans-membrane passive leak of charge which occurs in native SR membranes (except for transported Ca^{2+}). Ca^{2+} and H^+ concentrations and electrical potential were then measured with appropriate sensors (Fig. 5). It was found that addition of ATP was accompanied by Ca^{2+} uptake and stoichiometric H^+ extrusion, as well as formation of electrical potential.¹¹

The important role of H^+ at the Ca^{2+} sites was also demonstrated in experiments with native membrane vesicles, as it was found that phosphorylation of ATPase with P_i can be obtained only at acid pH. This indicates that upon 2H^+ binding to E_2 (in exchange for Ca^{2+} if present) the resulting $2\text{H}^+\cdot\text{E}_2$ acquires a specific conformation and free energy to allow phosphorylation with P_i , i.e. reversal of the $\text{E}_2\sim\text{P}\cdot 2\text{Ca}^{2+}$ to $2\text{H}^+\cdot\text{E}_2$ step in the ATPase reaction cycle.¹²

Pioneering and highly informative crystallography by Toyoshima et al. revealed detailed structural information on the molecular structure of the entire molecule.¹³ Nucleotide and phosphorylation domains of the Ca^{2+} ATPase, relative to different stages of the enzyme cycle, are represented in Fig 6.¹⁴ In the figure, the structure and conformational states of the Ca^{2+} ATPase in

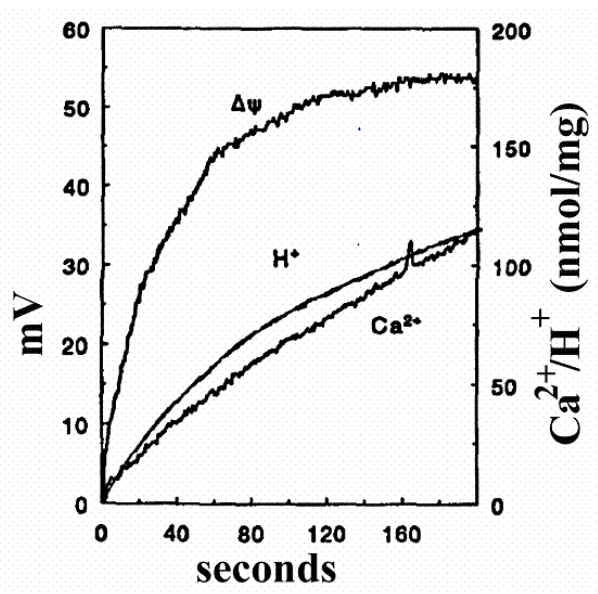


Figure 5. ATP dependent Ca^{2+} uptake, H^+ countertransport and development of transmembrane electrical potential in reconstituted SERCA proteoliposomes. The proteoliposomes were placed in a neutral pH medium, containing 100 mM K_2SO_4 , 50 μM CaCl_2 , and color reagents for detection of Ca^{2+} , pH and electrochemical gradients. The reaction was started by the addition of 0.2 mM ATP, and followed by differential absorption spectrometry.¹¹

the presence and absence of Ca^{2+} , substrate and product analogs are represented, with reference to E_1 , 2Ca^{2+} , $\text{E}_1\cdot\text{AMPPCP}$, $\text{E}\cdot 2\cdot\text{AIF4}\cdot(\text{TG})$, and $\text{E}_2\cdot(\text{TG})\cdot\text{ATP}$, where TG (thapsigargin, a highly specific and potent SERCA inhibitor) is used to stabilize E_2 .^{13, 15, 16, 17} Color changes gradually from the N-terminus (blue) to the C-terminus (red). The two Ca^{2+} (I and II) bound to the high affinity transmembrane site are circled when present. The two bound Ca^{2+} undergo vectorial release in $\text{E}_2\cdot\text{AIF4}\cdot(\text{TG})$, as the binding sites undergo a change in affinity and orientation. Three key residues (E183 in the A domain, D351 and D703 in the P domain) are shown in ball-and-stick. Note the positional change of headpiece domains in the various conformations. Note the nucleotide binding to the N domain, and variable relationship of the nucleotide phosphate chain (and Mg^{2+}) with the P and A domains.

As described above, kinetic and structural information yields a detailed understanding of the Ca^{2+} ATPase catalytic and transport cycle as outlined in Fig. 4.

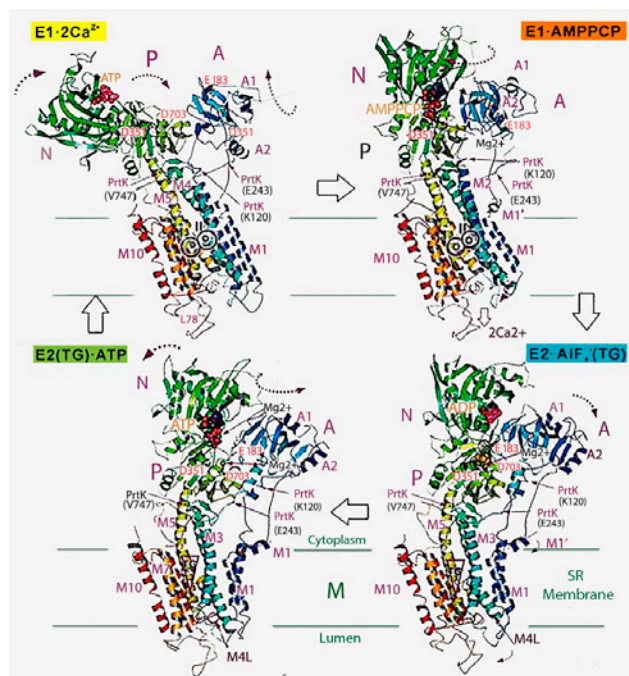


Figure 6. Sequence of conformational states of the calcium ATPase in the presence (E1.2Ca²⁺), following nucleotide (analog) substrate binding (E1-AMPPCP), following enzyme phosphorylation (AIF₄ analog) and Ca²⁺ release (E2.AIF₄.TG) and in absence of Ca²⁺ with bound ATP (E2(TG).ATP).¹⁴

THE COPPER TRANSPORT ATPASE

Bacterial and mammalian copper ATPases sustain active transport of copper by utilization of ATP. The mammalian Cu⁺ ATPases include isoforms (ATP7A and ATP7B) that are involved in copper transfer from enterocytes to blood, copper export from the liver to the secretory pathways for incorporation into metalloproteins, and general copper homeostasis.^{18,19} Genetic defects of ATP7A and ATP7B are related to human Menkes and Wilson diseases.^{20, 21, 22}

Cu²⁺ ATPases present functional analogies to the Ca²⁺ ATPases, but specific differences as well. A comparison of SERCA and ATP7B bidimensional folding models (Fig. 7) shows that ATP7B comprises eight (rather than ten) transmembrane segments that include the copper binding site (TMBS) for catalytic activation and transport, and a headpiece comprising the N, P and A domains with conserved catalytic motifs analogous to SERCA.

A specific feature of ATP7B (less prominent in ATP7A, and absent in the bacterial copper ATPase) is an amino-terminal extension (NMBD) with six copper binding sites in addition to those in the TMBS. An

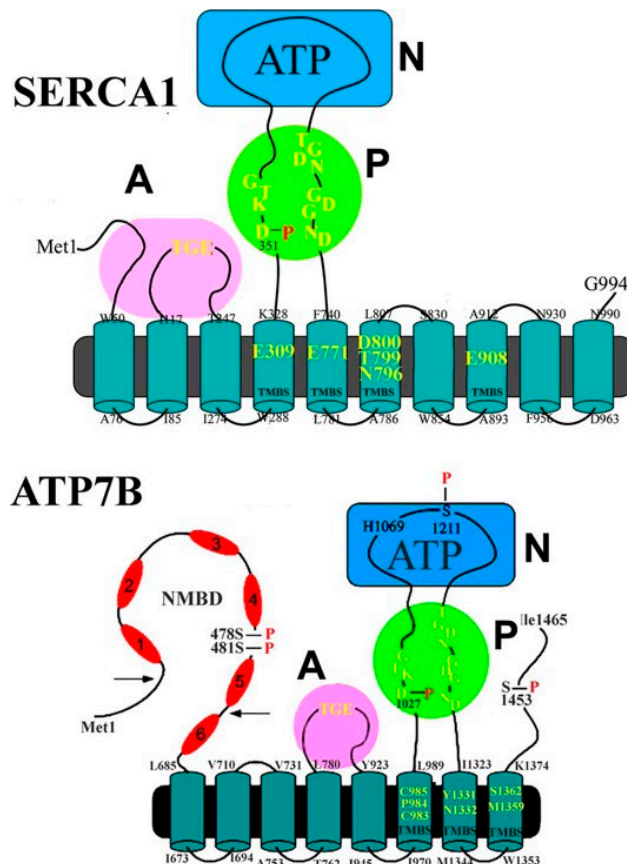


Figure 7. Two-dimensional folding models of the Ca²⁺ ATPase (SERCA1) and Cu⁺ ATPase (ATP7B) sequence. The diagram shows ten SERCA or eight ATP7B transmembrane domains including the calcium or copper binding sites (TMBS) involved in enzyme activation and cation transport. The extra-membranous regions of both enzymes comprises a nucleotide binding domain (N), the P domain with several conserved residues (in yellow) including the aspartate (Asp351 and Asp1027) undergoing phosphorylation to form the catalytic intermediate (EP), and the A domain with the TGE conserved sequence involved in catalytic assistance of EP hydrolytic cleavage. The His1069 residue whose mutation is frequently found in the Wilson disease is shown in the ATP7B N domain. Specific features of ATP7B are the N-metal Binding Domain (NMBD) extension with six copper binding sites, and serine residues undergoing Protein Kinase assisted phosphorylation (Ser478, Ser 481, Ser1211, Ser1453).²³

additional feature is the presence of serine residues (Ser-478, Ser-481, Ser1211, Ser-1453 in ATP7B) undergoing kinase assisted phosphorylation.²³

The native abundance of copper ATPase is quite low and, in order to accomplish biochemical experimentation, larger quantities were obtained by heterologous expression in insect or mammalian cells.^{24, 25} It was found that addition of ATP to microsomes expressing heterologous ATP7B yields two fractions of phosphoryl-

ated ATPase protein, one acid labile corresponding to phosphoenzyme intermediate, and the other acid stable and dependent on kinase assisted phosphorylation. Acid labile phosphoenzyme is faster, and is not observed following mutation of the conserved aspartate (S1024) at the catalytic site, or following mutation of the trans-membrane copper binding site (TMBD). Kinase assisted formation of alkali resistant phosphorylation is slower, involves Ser478, S481, Ser1121 and Ser1453, and is not observed in the presence of protein kinase inhibitors. Interestingly, it is not observed following mutation of the trans-membrane copper binding site (TMBD), indicating a dependence on enzyme activation (E_2 to E_1) transition.

Specific features of copper ATPase following addition of ATP are shown in Fig 8, to demonstrate the difference in phosphorylation of aspartate and serines in the copper ATPase. The time course of ATP7B following addition of ATP is shown in Fig 8A, with total phosphoenzyme (black squares) including acid and alkaline resistant (dark squares, including aspartate phosphoenzyme intermediate and phospho-serines), acid resistant (dark circles, i.e. aspartate phosphoenzyme intermediate) and alkaline resistant (light squares, i.e. phosphoserines). It is shown in Fig 8B that no alkaline resistant phosphoenzyme (i.e. phosphoserines, light squares) is observed if protein kinase inhibitor is present, and in Fig 8C no acid resistant aspartate phosphoenzyme (dark circles) is observed when D1027N ATP7B is used. By comparison, it is shown in Fig 8D that WT SERCA undergoes only acid stable aspartate phosphorylation, and no alkali resistant serine (light squares) phosphorylation, i.e. the acid stable accounts for total phosphorylation.²⁵

An estimate of Cu^{2+} transport following phosphorylation of ATP7B with ATP was obtained by comparing microsomes of COS-1 expressing Ca^{2+} ATPase (SERCA) or Cu^+ ATPase (ATP7B) absorbed on a solid supported membrane (SSM). The SSM consists of an alkanethiol monolayer covalently bound to a gold electrode via the sulfur atom and a phospholipids monolayer on top of it.^{26, 27, 28} The adsorbed protein is activated by addition of ATP in the presence of a medium supporting ATPase activity. Related electrogenic events are recorded as current transients due to flow of electrons along the external circuit toward the electrode surface, as required to compensate for the potential difference across the vesicular membrane produced by displacement of positive charge upon vectorial translocation in the direction of the SSM electrode. When ATP is added to the membrane bound ATPase absorbed on the SSM in the presence of Ca^{2+} or Cu^{2+} , a current transient is obtained due to vectorial translocation of bound Ca^{2+} or Cu^{2+} in the direction of the SSM electrode after phosphoenzyme

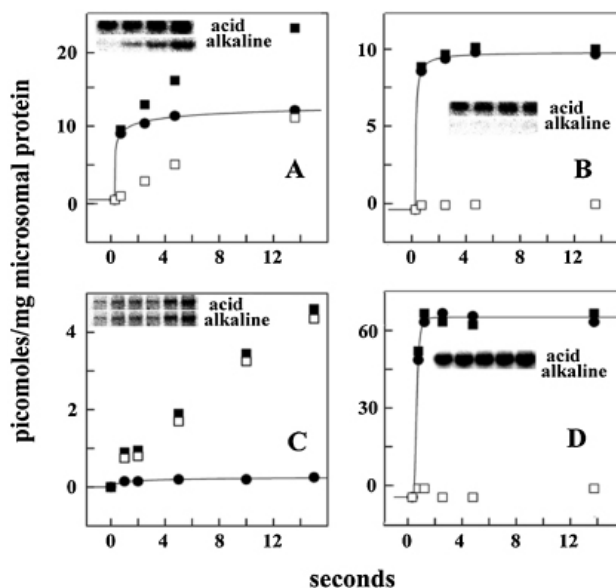


Figure 8. Phosphorylation of WT ATP7B (A, B), ATP7B D1027N mutant (C), and WT SERCA (D), in the absence (A, C and B) and in the presence of Proteinase K inhibitor. Microsomes obtained from COS-1 cells sustaining expression of the various ATPases were incubated with 50 microM (γ - ^{32}P)ATP in a reaction mixture sustaining enzyme activity at 30 °C, in the absence (A, C and D) or in the presence (B) of PKD inhibitor. Electrophoresis was then performed at acid pH to measure total phosphoproteins (black squares), or alkali pH to eliminate alkali labile phosphoenzyme and assess alkali resistant serine phosphorylation (empty squares). The difference (given in in the absence (A, C and D) or in the presence (B) of PKD inhibitor. Electrophoresis was then performed at acid pH to measure total phosphoproteins (black squares), or alkali pH to eliminate alkali labile phosphoenzyme and assess alkali resistant serine phosphorylation (solid black circles) corresponds to the phosphorylated aspartate enzyme intermediate.²⁵

formation by utilization of ATP. In these experimental conditions, the electrogenic signal generated within the first enzyme cycle is observed.²⁹ It is shown in Fig 9A that in experiments with SERCA that the charge transfer observed at neutral pH is much reduced at acid pH. On the other hand, the charge transfer observed with ATP7B is significantly slower, and is not changed by alkaline or acid pH (Fig 9B). This difference is due to the lack of $\text{Cu}^{2+}/\text{H}^+$ exchange in the cation binding and release sites of the copper ATPase, as opposed to the requirement of $\text{Ca}^{2+}/\text{H}^+$ exchange in the calcium ATPase.

A crystallographic view of the copper ATPase protein and of the copper transport pathway across the membrane was obtained through LpCopA crystallization, trapped in the $E_2\cdot\text{P}_i$, as compared with $E_2\text{P}$ state.³¹ The two states show the same conduit, appearing equivalent and open to the extracellular side, in contrast to the

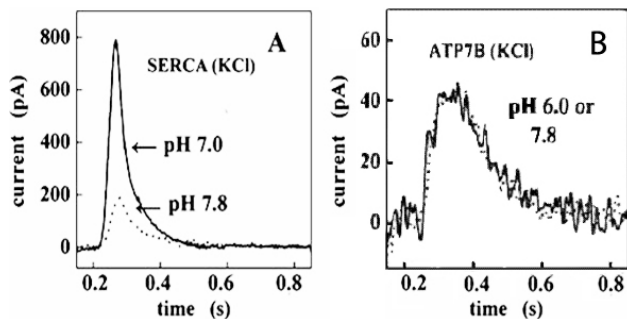


Figure 9. Charge measurements measured with enzymes absorbed on solid supports member (SSM). A: Current transients following addition of ATP to SERCA in a reaction mixture including 10 microM free Ca^{2+} and 100 mM KCl at pH 7.0 (solid line) or pH 7.8 (dotted lines). C: Current transients after addition to ATP on ATP7B in a reaction mixture containing 5 microM Cu^{+} and 100 mM KCl at pH 6.0 (solid line) or 7.8 (dotted line).²⁸

calcium ATPase where the E_2P_i state is occluded. In Fig 10a the A, P and N domains are colored in yellow, blue and red, respectively. The black arrows mark the copper transport pathway. In Fig 10b the E_2P (pink) and E_2P_i (green) states are compared, showing movements of the extracellular domains (arrows), while the transmembrane domain remains rigid in two states, in contrast to the calcium ATPase where the E_2P_i becomes occluded. Fig 10c shows a close up of the extrusion pathway with the opening from the copper high affinity coordinating residues Cys382, Cys384, and Met717 shown as a red surface, with crystallographic water molecule shown as red spheres.

A diagrammatic comparison of the calcium and copper ATPases is shown in Fig 11, where the sequential conformational transitions of the catalytic and transport cycle are compared for calcium and copper ATPases.³⁰ We then see that the two calcium ions exit the ATPase from the E_2P state, and the ion exit pathway closes concomitantly to hydrolytic cleavage of P_i and transition to the E_2P_i state. On the other hand, the copper ions exit the ATPase from the E_2P state, but the exit pathway remains open in the E_2P_i state, and closes only in the E_2 state after release of P_i .

Considering experimental results and modeling shown above, there seems to be a clear parallel between the difference in cation/proton exchange, and the conformational outcome in the exit pathways following cation release in the two ATPases. It is apparent that the closure of the release pathway in the calcium ATPase is due to H^+ binding in exchange for Ca^{2+} , and a consequent conformational effect on the E_2P_i state. The pathway closure in the copper ATPase occurs only following release of P_i and acquisition of the E_2 conformation.

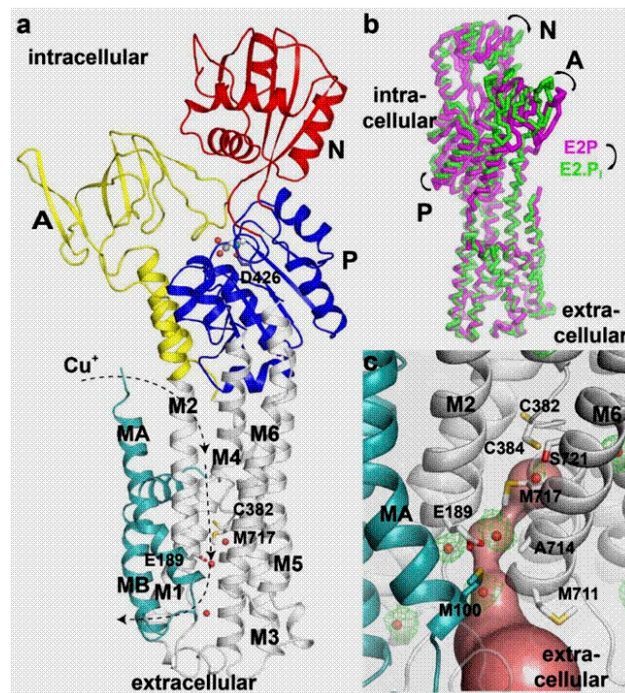


Figure 10. Diagrammatic representation showing that crystal waters of the $\text{E}_2\text{-BeF}_3^-$ structure support the copper release pathway.³⁰

A further distinctive feature of the copper ATPase is the effect of phosphorylation of serine residues catalyzed by Proteine Kinase D.²⁵ In experiments with microsomes of COS1 cells or hepatocytes expressing ATP7B it was found that utilization of ATP by ATP7B includes autophosphorylation of an aspartyl residue serving as the specific catalytic intermediate, as well as phosphorylation of serine residues catalyzed by Protein Kinase D. It is shown in Fig 12 A that ATP7B (stained in green) interacts first with TransGolgi network (blue) in perinuclear (nuclei red) location and, in the presence of Cu^{2+} , is transferred to intracellular trafficking vesicles. It is shown in Fig12 B that the trafficking is not interfered with by mutation of the TMBD Asp1027 (whose phosphorylation serves as phosphoenzyme intermediate). On the other hand, trafficking is interfered by Ser478, 481, 1121 and 1453 mutations in the NMD (Fig12C), by TMBS copper site mutation (Fig 12D), and by mutation of the 6th NMBD copper site mutation (Fig 12 E). This demonstrates that the NMD, absent in the calcium ATPase, plays a determinant role in conformational adaptations required for functions of the copper ATPase.

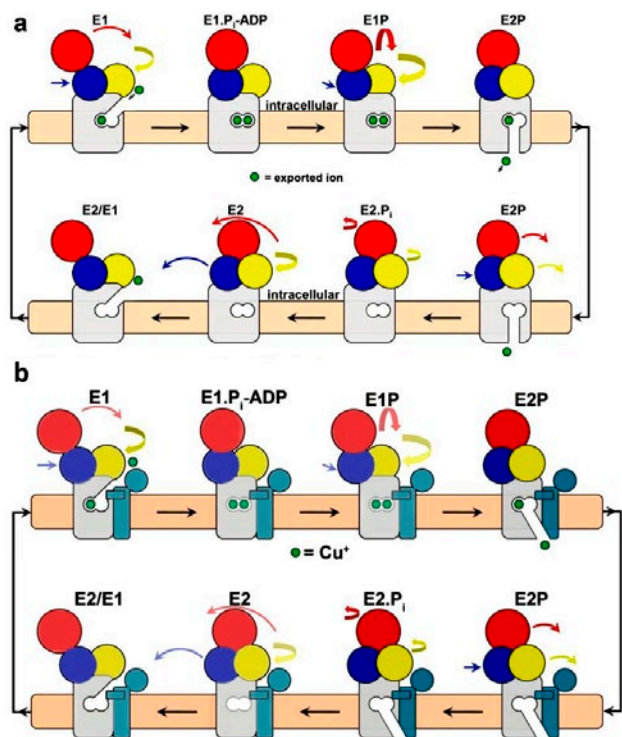


Figure 11. Diagrammatic comparison of the calcium and copper ATPases, showing the sequential conformational transitions of the catalytic and transport cycle. The two transported calcium ions exit the ATPase from the E2P state, and the ion exit pathway closes concomitantly to hydrolytic cleavage of Pi and transition to the E2.Pi state. On the other hand, the copper ions exit the ATPase from the E2P state, but the exit pathway remains open in the E2.Pi state, and closes only in the E2 state after release of Pi.³⁰

PHYSIOLOGICAL ROLES OF Ca^{2+} AND Cu^{+} ATPASES

Ca^{2+} is a specific activator of muscle fibrils. Activation of contraction depends on Ca^{2+} delivery and, in turn, and relaxation depends on reduction of Ca^{2+} concentration in the cytoplasm of skeletal and cardiac muscle cells. At rest, the cytosolic concentration of Ca^{2+} is much lower than in extracellular fluids and in the intracellular vesicles of sarcoplasmic reticulum. Muscle activation occurs when plasma membrane electrical action potentials open passive Ca^{2+} channels, allowing flux of Ca^{2+} in the cytosol for activation of myofibrils. Following the end of action potential, passive channels close, and cytosolic Ca^{2+} is returned to extracellular fluids and to the sarcoplasmic reticulum interior through active transport by the Ca^{2+} ATPase. Due to time limits and quantities of Ca^{2+} available, passive fluxes and active transport across the sarcoplasmic reticulum membrane are much prevalent over those across the outer plasma membrane. In the diagram on Fig 13, a cardiac myocyte

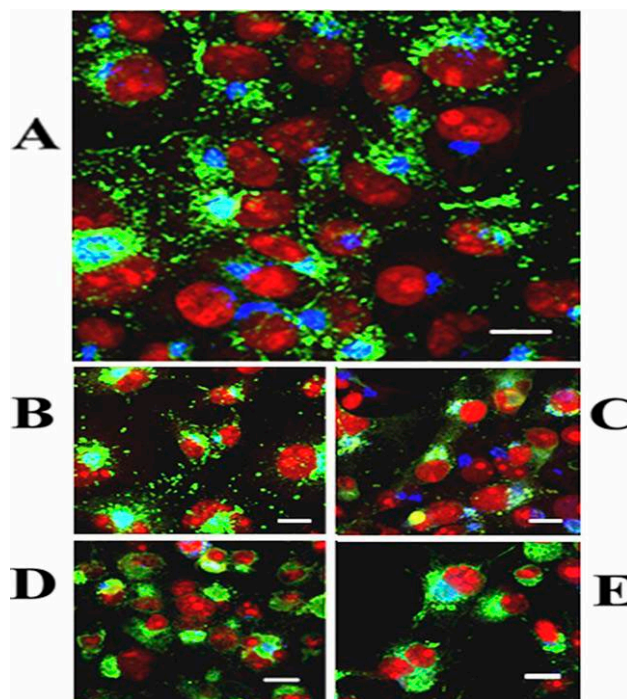


Figure 12. Intracellular distribution of ATP7b in COS1 cells expressing WT enzyme (A), subjected to mutation at Asp-1027 (B), Ser-478, Ser-481, Ser-1121 and SER-1453 (C), at the transmembrane (TMBD) copper site (D), or at the sixth NMBD copper site (E). Note the presence of cytosolic trafficking vesicles with WT enzyme (A), and even and even following Asp-1027 mutation (B), but no trafficking following serine, NMBD or TMBD copper sites (C, D and E).^{25, 29}

is shown with the Ca^{2+} ATPase (ATP) inserted in the plasma membrane (sarcolemma) and the sarcoplasmic reticulum membrane, collecting Ca^{2+} to induce relaxation, and to be then released upon membrane excitation to induce contraction upon binding to myofibrils.³¹ The inset shows the time course of an electrical action potential, Ca^{2+} release, and occurrence of contraction. Channels for passive diffusion of Ca^{2+} , and mitochondria are also shown.

Copper is a required metal for homeostasis of plants, bacteria and eukaryotic organisms, determining conformation and activity of many metalloproteins and enzyme such as cytochrome oxidase and superoxide dismutase. Furthermore, due to possible reactivity with non-specific proteins and toxic effects, elaborate systems of absorption, concentration buffering, delivery of specific protein sites and elimination, require a complex system including small carriers, chaperones and active transporters. The P-type copper ATPases provide an important system for acquisition, active transport, distribution and elimination of copper. A diagram of copper distribution in eukaryot-

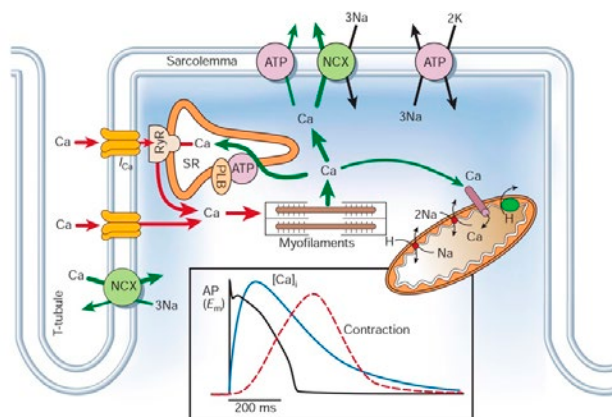


Figure 13. Ca^{2+} transport in ventricular cardiac myocytes. ATP: ATPase. NCX: $\text{Na}^+/\text{Ca}^{2+}$ exchange, SR: sarcoplasmic reticulum. Bers DM. Cardiac excitation-contraction coupling.³¹ *Nature* 2002; 415 :198-205

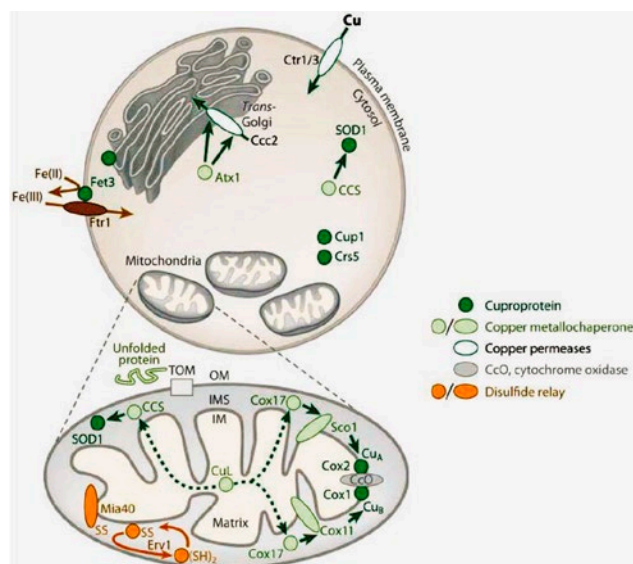


Figure 14. Diagram of copper eukaryotic cellular distribution. See text for explanations.³²

ic cells is given in Fig. 14, where it is shown that copper is imported into the cells copper permeases (Ctr1: oval cell membrane bound circles).³²

Incoming Cu^{2+} does not remain free in the cytosol, but is rather bound to various chaperones delivering it to specific proteins and secretory pathway. The Cu^{2+} ATPase (Ccc2 in the figure with the trans-Golgi-Network) binds Cu^{2+} through the intervention of the Atx1 chaperone for delivery and transport across the cell membrane, or other destination depending on cell specificity. Cu^{2+} delivery to the cytochrome c oxidase

complex (CcO) involves Cox11, Sco1 and Cox 17 chaperones. Nuclear encoded chaperone proteins are imported unfolded across the mitochondrial membrane by a translocase, and then acquired in the inner mitochondrial space following introduction of disulphide bonds with the intervention of specific coupled enzyme.

In summary, it is evident that Ca^{2+} and Cu^{2+} ATPases are indispensable components of physiological systems, and the chemistry of their catalytic and transport mechanism is linked to biological function. Transport ATPases are required to regulate the concentrations of Ca^{2+} and Cu^{2+} within cells and cellular compartments, utilizing the energy of ATP to sustain appropriate concentrations across membranes. Appropriate cation concentrations are required to activate specific enzymes in one direction, and to produce relaxation and avoid toxic consequences in the other direction.

REFERENCES

1. R.W. Albers, *Ann. Rev. Biochem.* **1967**, 36, 727-756.
2. R.L. Post, C. Hegyvary, S. Kume, *J. Bio. Chem.* **1972**, 247, 6530.
3. L. de Meis, A. Vianna, *Ann. Rev. Biochem.* **1979**, 48, 275.
4. G. Inesi, *J. Cell Commun Signal* **2011**, 5, 227.
5. D.H. MacLennan, C.J. Brandl, B. Korczak, N.M. Green, *Nature* **1985**, 316, 696.
6. D.M. Clarke, T.W. Loo, G. Inesi, D.H. MacLennan *Nature* **1989**, 339, 476.
7. J. P. Anderssen, B. Vilsen, *FEBS Letters* **1995**, 359: 101.
8. D. Scales, G. Inesi, *Biophys J.* **1976**, 16, 735.
9. G. Inesi, M. Kurzmack, C. Coan, D. Lewis, D., *J. Biol. Chem.* **1980**, 255, 3025.
10. S. Verjovski-Almeida, M. Kurzmack, G. Inesi, *Biochemistry* **1978**, 17, 5006.
11. L. Hao, J.L. Rigaud, G. Inesi, *J. Biol. Chem.* **1994**, 269, 14268.
12. L. deMeis, G. Inesi, *Biochemistry* **1985**, 24, 922.
13. C. Toyoshima, M. Nakasako, H. Nomura, H. Ogawa. *Nature* **2000**, 405, 647.
14. G. Inesi, D. Lewis, H. Ma, A. Prasad, C. Toyoshima, *Biochemistry* **2006**, 45, 13769.
15. C. Toyoshima, T. Mizutani, *Nature* **2004**, 430, 529.
16. C. Olesen, T.L. Sorensen, R.C. Nielsen, J.V. Moller, P. Nissen, *Science* **2004**, 306, 2251.
17. A.L. Jensen, T.L. Sorensen, V. Olesen, J.V. Moller, P. Nissen, *The EMBO Journal* **2006**, 25, 2305.
18. J.M. Arguello, S.J. Patel, J. Quintana, *Matallomics* **2016**, 8, 906.

19. S. Lutsenko, N.L. Barnes, M.Y. Bartee, O.Y. Dmitriev, *Physiol Rev.* **2007**, 87, 1011.
20. C. Vulpe, B. Levinson, S. Whitney, S. Packman, J. Gitschier, *Nat. Genet* **1993**, 7, 13.
21. J.D. Gitlin, *Gastroenterology.* **2003**, 125, 1868.
22. M. Harada, *Med. Electron. Microsc.* **2002**, 35, 61.
23. R. Pilankatta, D. Lewis, C. M. Adams, G. Inesi, *J. Biol. Chem.* **2009**, 284, 21207.
24. Y.H. Hung, M.J. Layton, I. Voskoboinik, J. F. Mercer, J. Camakaris, *Biochem J.* **2007**, 401: 569.
25. R Pilankatta, D. Lewis, G. Inesi. *J.Biol Chem* **2011**, 286, 7389.
26. J. Pintschovius, K. Fendler, E. Bamberg, *Biophys. J.* **1999**, 76, 827.
27. F. Tadini-Buoninsegni, G. Bartolommei, M.R. Moncelli, R. Guidelli, G. Inesi, *J. Biol. Chem.* **2006**, 281, 37720.
28. G. Tadini-Buoninsegni, G. Bartolommei, M.R. Moncelli, R. Pilankatta, D. Lewis, G. Inesi, *FEBS Lett.* **2010**, 584, 4519.
29. D. Lewis, R. Pilankatta, G. Inesi, G. Bartolommei, M. R. Moncelli, F. Tadini-Buoninsegni, *J. Biol. Chem.* **2012**, 287, 32717.
30. M. Andersson, D. Mattle, O. Sitsel, A.M. Nielsen, S. H.White, P. Nissen, P. Gourdon, *Nat. Struct. Mol. Biol.* **2013**, 21: 43-48.
31. M.D. Bers, *Nature* **2002**, 415, 198.
32. N.J. Robinson, D.R. Winge, *Annual Rev. Biochem.* **2010**, 79, 537.